Chinese Journal of
POLYMER SCIENCE

ARTICLE

https://doi.org/10.1007/s10118-018-2065-3
Chinese J. Polym. Sci. 2018, 36, 783–790

Fully Biodegradable Poly(lactic acid)/Poly(propylene carbonate) Shape Memory Materials with Low Recovery Temperature Based on *in situ* Compatibilization by Dicumyl Peroxide

Sheng-Xue Qin[a, b], Cui-Xiang Yu[a], Xue-Yang Chen[a], Hai-Ping Zhou[a*], and Li-Fen Zhao[a*]

[a] *College of Mechanical and Electric Engineering, College of Materials Science and Engineering, Shandong University of Science and Technology, Qingdao 266590, China*
[b] *Qingdao Reinforced Thermoplastic Pipes Engineering Technology Center, Qingdao 266590, China*

Abstract Fully biodegradable blends with low shape memory recovery temperature were obtained based on poly(lactic acid) (PLA) and poly(propylene carbonate) (PPC). By virtue of their similar chemical structures, *in situ* cross-linking reaction initiated by dicumyl peroxide (DCP) between PLA and PPC chains was realized in PLA/PPC blends. Therefore, the compatibility between PLA and PPC was increased, which obviously changed the phase structures and increased the elongation at break of the blends. The compatibilized blends had a recovery performance at 45 °C. Combining the changes of phase structures, the mechanism of the shape memory was discussed. It was demonstrated that *in situ* compatibilization by dicumyl peroxide was effective to obtain eco-friendly PLA/PPC blends with good mechanical and shape memory properties.

Keywords Polylactide; Poly(propylene carbonate); Dicumyl peroxide; Compatibilization; Shape memory

Citation: Qin, S. X.; Yu, C. X.; Chen, X. Y.; Zhou, H. P.; Zhao, L. F. Fully Biodegradable Poly(lactic acid)/Poly(propylene carbonate) Shape Memory Materials with Low Recovery Temperature Based on *in situ* Compatibilization by Dicumyl Peroxide. Chinese J. Polym. Sci. 2018, 36(6), 783–790.

INTRODUCTION

Biodegradable shape memory polymers (SMP) have attracted great attention in recent years because of their potential use in biomedical fields, such as stents, sutures, drug delivery carriers and wound healing materials[1–4]. As a most promising biodegradable polymer, poly(lactic acid) (PLA) with good biocompatibility and biodegradability has also been used to prepare shape memory materials[5, 6]. In most cases, the shape memory property of PLA is triggered by heating. PLA sample with original shape is usually heated to a transition temperature (T_s) above the glass transition temperature (T_g, about 60 °C). A temporary shape is obtained at T_s by a load and then the temperature is lowered below T_g. After releasing the load, the temporary shape with low entropy is fixed. When the deformed sample is reheated to T_s, the original shape can be recovered by the entropy driving force.

From above shape memory process, it is found that the recovery temperature of PLA is higher than that of human body, which limits its usage as SMP in biomedical field. Besides that, the inherent brittleness of PLA also limits its applications as SMP in other fields[7, 8]. Blending is an effective way to overcome the brittleness and to decrease the shape memory temperature. Many polymers with low glass transition temperature, such as thermoplastic polyurethane (TPU)[9], polyamide elastomer (PAE)[10] and natural rubber (NR)[11], have been blended with PLA to prepare SMP. However, in these reported studies, the recovery temperatures of these blends are all above 60 °C.

Poly(propylene carbonate) (PPC) is a biodegradable polymer that can be obtained by copolymerization of carbon dioxide (CO_2) and propylene oxide. Because of CO_2 use, PPC has attracted great interests since appeared[12–17]. Moreover, it shows good properties such as ductility, biocompatibility and low glass transition temperature (about 35 °C), which could be used to improve the toughness of PLA[18–20]. Unfortunately, the poor compatibility of PLA and PPC is a critical obstacle for the improvement of the properties of the blends[21]. To overcome this difficulty, introduction of a copolymer (block, graft, or star) or a reactive modifier, including poly(vinyl acetate) (PVAc), maleic anhydride (MA), has been carried out[21–26]. However, to the best of our knowledge, there is still no reported work available with regard to the studies on the shape memory of the outcome materials.

The aim of this work is to obtain SMP with low recovery temperature by PLA/PPC blending. For SMP based on polymer blends, cross-linking structure has a positive effect

* Corresponding authors: E-mail zhouhp325@163.com (H.P.Z)
E-mail lfzhao2009@126.com (L.F.Z)
Received September 5, 2017; Accepted October 17, 2017; Published online January 30, 2018

on improving their shape memory properties by supplying high resilience[27–29]. Furthermore, cross-linking is a valid method to improve the compatibility between different blends. It was reported that the compatibility of biodegradable poly(ε-caprolactone)/polylactic acid (PCL/PLA) and poly(butylene adipate-*co*-terephthalate)/polylactic acid (PBAT/PLA) blends was improved significantly by dicumyl peroxide (DCP) initiated cross-linking[30, 31]. Inspired by these works, DCP was chosen as the *in situ* cross-linking agent in PLA/PPC blend for the first time to improve the compatibility and shape memory properties simultaneously. The changes of phase structures, mechanical and shape memory properties brought by the cross-linking reaction were investigated. It is expected that this work will give some inspirations on the design of fully biodegradable shape memory materials useful in biomedical fields.

EXPERIMENTAL

Materials

PLA with $M_w = 2.5 \times 10^5$ g/mol (2002D) was purchased from Nature-Works (USA). PPC with $M_w = 6.14 \times 10^4$ g/mol was purchased from Nanyang Zhongju Tianguan Low Carbon Technology Co. Ltd. (Henan, China). Their chemical structures are presented in Scheme 1. DCP used in this study was obtained from Shanghai Shanpu Chemical Co. Ltd (Shanghai, China). Before being used, PLA and PPC were dried in a vacuum oven for 72 h to remove residual moisture.

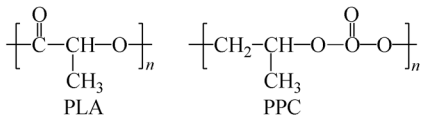

Scheme 1 Chemical structures of PLA and PPC

Sample Preparation

PLA/PPC blends were prepared by melt blending in a XSS-300 torque rheometer (Shanghai Kechuang Rubber Machinery Equipment Co. Ltd, China). The blends of PLA/PPC, with weight ratio of 100/0, 90/10, 80/20, 70/30 and 60/40, were prepared at 170 °C. Different amounts of DCP (0, 0.5 wt%, 1.0 wt%, 1.5 wt% and 2.0 wt%) were added into the blends with PLA/PPC of 70/30 in order to prepare the sample with cross-linked structure. All samples after blending were moulded at 170 °C with a pressure of 10 MPa prior to the subsequent procedure.

Characterization

FTIR analysis

Fourier transform infrared (FTIR) spectra for all the samples were obtained at constant spectral resolution of 2 cm^{-1} using an FTIR spectrometer (Nicolet 380, USA) at 25 °C.

Differential scanning calorimetry

Differential scanning calorimeter (Mettler-Toledo, TGA/DSC1/1600LF, Switzerland) was used to meaure the glass transition temperature (T_g) and melting temperature (T_m) under nitrogen at a flow rate of 20 mL/min. In a typical program, the sample was first heated to 200 °C at a heating rate of 10 K/min and held at 200 °C for 2 min to eliminate the effect of thermal history. After that, the sample was quenched to 0 °C and heated to 200 °C again at the heating rate of 10 K/min.

Gel fraction

A blend sample was dissolved in chloroform for 24 h, and submitted to Soxhlet extraction to remove linear PLA or PPC. The insoluble part of the sample, estimated as the cross-linked polymer, was dried in the oven at 50 °C for 24 h. The gel fraction was evaluated using the following Eq. (1)[32]:

$$\text{Gel} = W_g/W_0 \times 100\% \quad (1)$$

where Gel is the gel fraction of the sample, W_g is the weight of the dried insoluble part of the sample after extraction, and W_0, the original weight of the sample.

Tensile test

The tensile properties were tested with an AL-7000M tensile testing machine (Gaotie Detection Equipment Co. Ltd, China) with a cross-head speed of 20 mm/min at room temperature (around 25 °C). The samples were cut into dumbbell-shape with the dimension of 4 mm in width (the narrow section), 1.0–1.3 mm in thickness and 75 mm in length. The averaged values of the results obtained from five samples for each blend composition were reported.

Scanning electron microscopy

All the samples were fractured in liquid nitrogen and etched with an anhydrous ethanol/acetone (1/1, *V*/*V*) mixed solution to remove partially PLA in a shaking water bath for 1 min. After drying at 30 °C for 24 h in an oven, the samples were coated with gold in vacuum to be observed by a scanning electron microscope (Nova Nano SEM 450, FEI Company, USA) with an acceleration voltage of 10 kV.

Shape memory properties

The shape recovery ratio of the samples was examined by a stretching test with a tension meter (HP-200N, Leqing Aidebao Instrument Co. Ltd, China). PLA/PPC/DCP blend samples were cut into rectangular strips with the dimension of 50 mm × 7 mm × 1 mm. Gauge length of the samples is 30 mm (L_0). The sample was first stretched to make the gauge length change to about 60 mm (± 10%) with the aid of an external load in a water bath at 60 °C. After that, the sample was quickly transferred to another water bath at about 15 °C with the external load and held for 1 min to fix the shape (L_1). Subsequently, the deformed sample was transferred to the water bath with different temperatures to get recovery. After 20 min, the gauge length was recorded as L_2. The shape recovery ratio (Rr) was evaluated by Eq. (2):

$$R\text{r} = (L_1 - L_2)/(L_1 - L_0) \times 100\% \quad (2)$$

The shape recovery rate at the same temperature was examined by a bending test. PLA/PPC/DCP blend samples were cut into rectangular strips with the dimension of 50 mm × 7 mm × 1 mm. The samples were first folded in half in a water bath at 60 °C, and quickly transferred to another water bath at about 15 °C to fix the shape. After that, the deformed samples were transferred to a water bath at 45 °C and the shape recovery process was recorded with a digital camera.

https://doi.org/10.1007/s10118-018-2065-3

RESULTS AND DISCUSSION

Effect of DCP on the Compatibility of PLA/PPC Blends

The interaction of PLA/PPC blends was examined by FTIR. Figure 1 shows the FTIR spectra of PLA/PPC blends of different weight ratios. Because their chemical structure (Scheme 1) is very similar, their typical bands show little difference. For example, both PLA and PPC show their vibration peaks of hydroxyl and carbonyl at 3480 and 1760 cm^{-1}. Their distinct difference is observed in the wavenumber range from 1400 cm^{-1} to 700 cm^{-1} (Fig. 1b). One difference is the peak of —CH unsymmetrical bending vibration[33]. For pure PLA, the peak appears at 1364 cm^{-1}. With increasing the content of PPC, it shifts to the lower wavenumbers and locates at 1356 cm^{-1} for the neat PPC sample. The other difference is the peak at 869 cm^{-1}, ascribed to the C—C peak of PLA[34]. It is also shifted significantly towards lower wavenumber with the increase of PPC content. The shifting of these typical bands for PLA and PPC indicates that there exist some specific interactions between PLA chains and PPC chains, which are helpful to enhance their compatibility.

To further investigate the compatibility of PLA/PPC blends, the T_g data were collected by differential scanning calorimetry (DSC). Figure 2 shows the DSC traces of PLA/PPC blends and the corresponding thermal parameters are given in Table 1. For pure PLA and PPC, the T_g value was about 60 and 36 °C, respectively. However, two T_gs were observed in the PLA/PPC blends with different weight ratios. For example, in PLA/PPC 60/40 blend, the T_g at high temperature corresponding to the T_g of PLA was 57 °C, which was 3 °C lower than that of neat PLA. In PLA/PPC 80/20 blend, T_g at low temperature corresponding to that of PPC was 38 °C, which was 2 °C higher than that of neat PPC. The T_g shifting towards each other in the blends suggests that PLA/PPC blends were a partially compatible system, which is in agreement with the results of FTIR shown in Fig. 1. This partial compatibility can be attributed to their similar chemical structures of the two polymers.

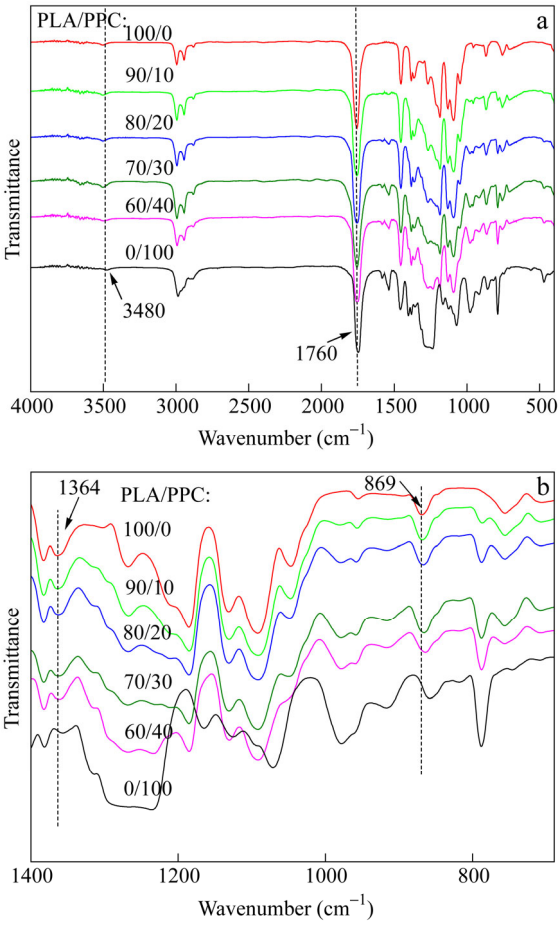

Fig. 1 FTIR spectra of PLA/PPC blends with various blending ratios: (a) the spectra in the wavenumber range from 4000 cm^{-1} to 400 cm^{-1}; (b) enlarged FTIR spectra in the wavenumber range from 1400 cm^{-1} to 700 cm^{-1}

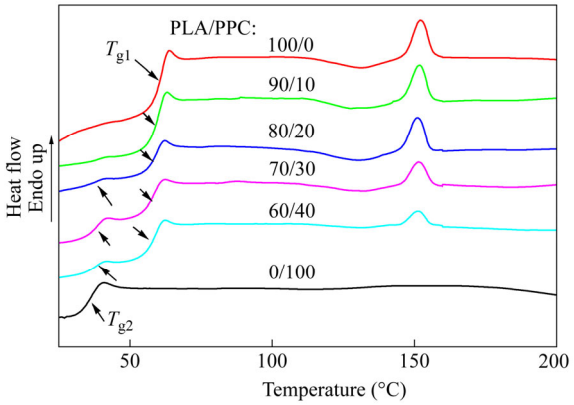

Fig. 2 DSC heating curves at 10 K/min for PLA/PPC blends with various blending ratios

Table 1 Thermal parameters of PLA/PPC blends

PLA/PPC	T_{g1} (°C)	T_{g2} (°C)	T_m (°C)	ΔH (J/g)
100/0	60.0	–	152.2	1.83
90/10	59.8	38.0	151.8	1.57
80/20	59.5	37.9	151.2	1.42
70/30	58.5	37.1	151.2	1.28
60/40	57.0	36.5	151.5	0.98
0/100	–	36.0	–	0

In order to increase the compatibility of PLA to PPC in their blends, DCP was incorporated into PLA/PPC 70/30 blend to investigate the cross-linking effect on the compatibility of the blend. Figure 3 illustrates the FTIR spectra of this blend with different DCP contents. The most significant change was observed for the —O—C—O— stretching vibration peak at 1228 cm^{-1}[35]. The addition of DCP into this PLA/PPC blend enhanced the intensity of this peak, and the position of the peak shifted to a high wavenumber by 5 cm^{-1} when the DCP concentration varied from 0 wt% to 2 wt%. This indicated that some cross-linking was formed between the chains of PLA and PPC with DCP incorporated into the blend.

DSC study was also carried out to study the compatibility of PLA/PPC/DCP blends. Figure 4 and Table 2 show the results of the blends with different DCP contents. The T_g at the high temperature region corresponding to that of PLA was

https://doi.org/10.1007/s10118-018-2065-3

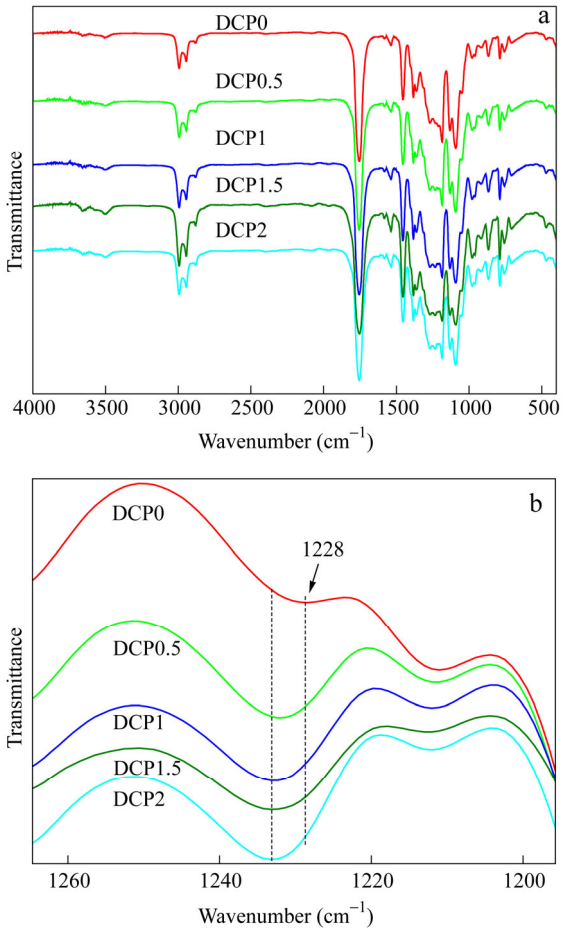

Fig. 3 FTIR spectra of PLA/PPC/DCP with various DCP contents: (a) the spectra in the wavenumber range from 4000 cm^{-1} to 400 cm^{-1}; (b) enlarged FTIR spectra in the wavenumber range from 1280 cm^{-1} to 1180 cm^{-1}

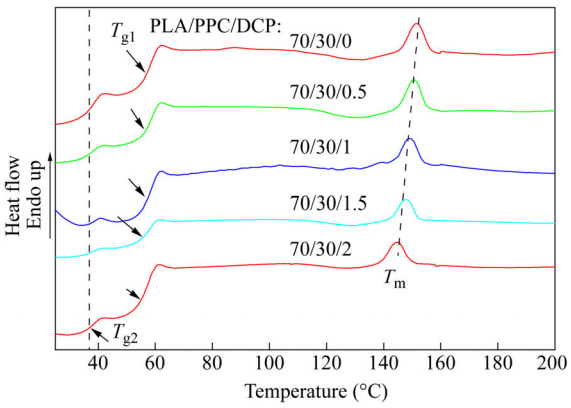

Fig. 4 DSC heating curves of PLA/PPC/DCP: 70/30/0, 70/30/0.5, 70/30/1, 70/30/1.5, 70/30/2 (The heating rate was 10 K/min.)

Table 2 Thermal parameters of PLA/PPC/DCP samples

PLA/PPC/DCP	T_{g1} (°C)	T_{g2} (°C)	T_m (°C)	ΔH (J/g)
70/30/0	58.0	37.0	151.2	1.28
70/30/0.5	57.5	37.0	150.5	1.16
70/30/1	57.1	37.0	149.0	1.04
70/30/1.5	56.5	37.0	147.7	0.91
70/30/2	55.0	37.0	145.0	0.90

at about 58 °C in PLA/PPC 70/30 sample. For the sample with 2 wt% DCP, it decreased to 55 °C. Meanwhile, the T_g corresponding to that of PPC for all the samples was at about 37 °C. There are two possibilities which caused this shift towards each other in the PLA/PPC/DCP blends. The first was the cross-linking reaction happened between the PLA and PPC chains, which would increase their compatibility and decrease the T_g of PLA in the samples. However, the unchanged T_g of PPC suggested that there was degradation reaction accompanying the cross-linking reaction. Therefore, there was the second possibility. The cross-linking reaction happened mainly between the chains of the two homopolymers. Because of the unavoidable degradation reaction brought by the introduction of DCP radical initiator, the decrease of T_g for PLA or unchanged T_g for PPC might happen. Furthermore, the melting peaks of PLA shifted to lower temperature region with the increase of DCP content as shown in Fig. 4. The decrease of these melting peaks indicated that the crystallization of PLA was influenced by the cross-linking brought by DCP. However, it is difficult to determine the exact structure of the cross-linking.

In order to further explore the structures of PLA/PPC/DCP, the fracture morphology was investigated by SEM (Fig. 5). All the samples were etched in a mixed solution of anhydrous ethanol and acetone in a shaking water bath to better analyze the morphology. From Fig. 5(a), we can see that PLA/PPC 70/30 blends exhibited typical "sea-island" morphology, in which PPC domains with a diameter of about 10 μm were dispersed in the PLA matrix. In the outlined region, it is observed that there were some void region between the "island" and the "sea", which suggests again that the PLA and PPC was not well compatible. When 0.5 wt% of DCP was incorporated in the blend (Fig. 5b), the sizes of dispersed phase of PPC decreased to about 5 μm in diameter, although the "sea-island" morphology was still observed. Moreover, there were some linkages between the "sea" and "island", as pointed by the arrow signs. Interestingly, when DCP content reached 1 wt% (Fig. 5c), the dispersed PPC phase formed irregular shape and the phase interface was not very clear. When DCP content was increased to 1.5 wt% or 2 wt% (Figs. 5d and 5e), the distinct dispersed phase structure disappeared. Especially for the sample with 2 wt% of DCP, homogenous phase morphology was observed. The decrease of dispersed phase size, the linkage between the continuous and the dispersed phases, the irregular dispersed phase and even disappearance of dispersed phase all suggested that the loading of DCP improved the compatibility between PLA and PPC. In other words, compared with cross-linking reactions in PLA or PPC homopolymer, the reaction between the chains of PLA and PPC dominated and displayed a significant influence on the structures of the blends. Therefore, taking into account the results from FTIR, DSC and the changing of phase morphology, it can be concluded that the cross-linking structure between PLA and PPC chains was indeed formed in PLA/PPC/DCP blends, which resulted in the great changes of the compatibility and the phase structure.

In order to verify the above conclusion, gel in PLA/PPC/DCP blends was collected by a Soxhlet extractor with chloroform as the reflux solvent. Gel fraction of the

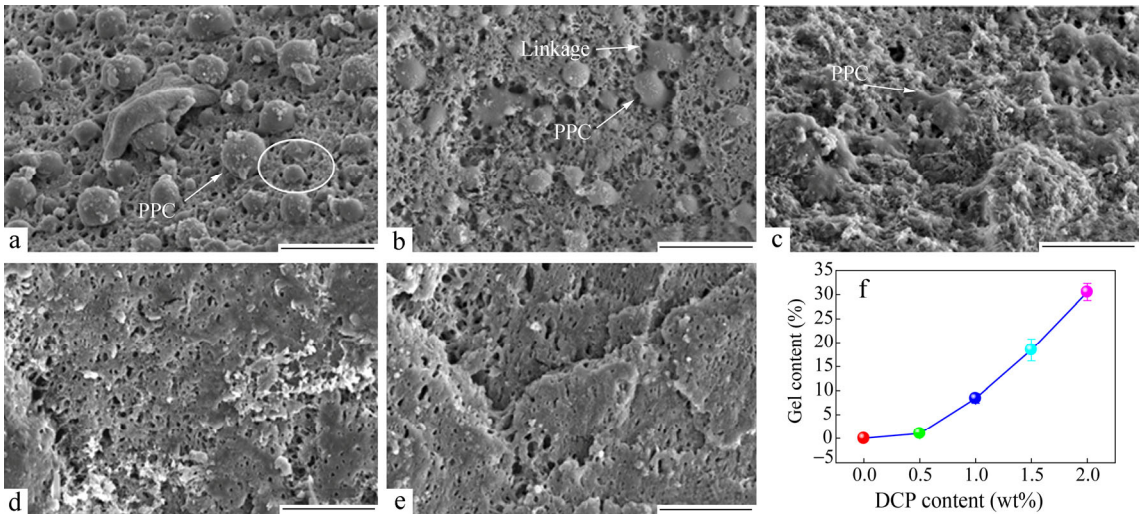

Fig. 5 SEM images for (a) PLA/PPC/DCP 70/30/0, (b) PLA/PPC/DCP 70/30/0.5, (c) PLA/PPC/DCP 70/30/1, (d) PLA/PPC/DCP 70/30/1.5, and (e) PLA/PPC/DCP 70/30/2 cryogenically fractured surfaces etched by mixed solvents of ethanol and acetone (The scale bar is 20 μm.); (f) Gel fraction of PLA/PPC/DCP blends with different amounts of DCP

simple blend of PLA and PPC was displayed in Fig. 5(f) along with the blends incorporated with different amounts of DCP. It can be seen that the gel fraction of the blends significantly rises from 0% to 36% with the amount of DCP increased from 0 wt% to 2 wt%. Because the content of PPC in the blends is 30%, the 36% of gel indicated again that cross-linking reactions happened between chains of PPC and PLA.

Mechanical Properties and Shape Memory Properties of the PLA/PPC/DCP Blends

Figure 6 illustrates the stress-strain relationship for the PLA/PPC/DCP blends and Table 3 gives the detailed data. From Fig. 6, it is seen that all the samples (with and without DCP) exhibited typical ductile tensile behavior with a yield strength above 45 MPa. When the DCP content was 1 wt% or lower, the elongation at break increased from 40% (PLA/PPC 70/30) to 107% (PLA/PPC/DCP 70/30/1), an increase of about 2 times compared with their original binary blends. However, the elongation at break dropped quickly when the content of DCP was above 1 wt%. Combining the gel fraction in Fig. 5(f) and the morphology shown in SEM images in Fig. 5, the increase of elongation can be attributed to the increase of compatibility of PLA and PPC. The decrease of elongation at break might be caused by excessive cross-linking, leading to a decrease in chain mobility. In general, the cross-linking would enhance the strength. Therefore, the almost unchanged tensile strength for blend with and without DCP was very unusual. It reminds us again that the degradation reaction, accompanying the cross-linking reaction in PLA/PPC/DCP samples, might contribute to the decreased strength when DCP content was higher than 1 wt%.

To further investigate the effect of the cross-linking on the shape memory performance, the *R*r data obtained from Eq. (2) versus DCP content at different recovery temperatures are shown in Fig. 7. It is seen that *R*r decreased with decreasing recovery temperature. When the recovery temperature was 60 and 55 °C, the shape recovery ratio was almost 100% for all the samples. With the recovery temperature decreased to 50 or 45 °C, *R*r decreased obviously. While the recovery temperature was set as 40 °C, the shape recovery performance

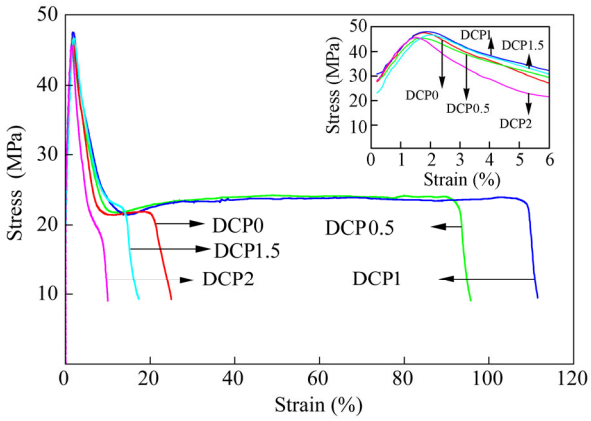

Fig. 6 Stress-strain curves of PLA/PPC blends with different DCP contents (The inset shows the enlarged curves with the strain below 10%.)

Table 3 Mechanical properties of PLA/PPC/DCP blends with different DCP contents

PLA/PPC/DCP	Young's modulus (MPa)	Yield strength (MPa)	Tensile strength (MPa)	Elongation at break (%)
70/30/0	1461 ± 200	47 ± 2	23 ± 1	40 ± 15
70/30/0.5	1496 ± 230	46 ± 3	23 ± 1	98 ± 13
70/30/1	1501 ± 130	48 ± 2	23 ± 1	107 ± 4
70/30/1.5	1527 ± 100	47 ± 2	21 ± 2	17 ± 5
70/30/2	1553 ± 100	46 ± 3	21 ± 2	15 ± 5

https://doi.org/10.1007/s10118-018-2065-3

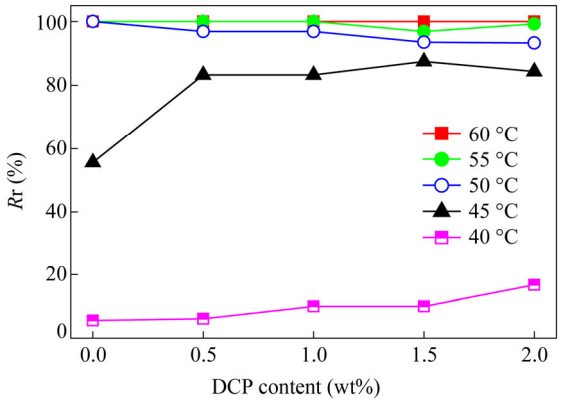

Fig. 7 Recovery ratio (*R*r) of PLA/PPC with various DCP contents

disappeared. It is easy to understand the recovery behaviors above 50 °C (T_g of PLA); the movement of both amorphous PLA and PPC chain segments driven by entropy increase provided well shape memory performance. When the recovery temperature decreased below the T_g of PLA, is there only the movement of PPC chains to provide *R*r? By comparing the *R*r values at 45 °C with different DCP contents, it was found that recovery ratio of PLA/PPC blends without DCP was 50%. While increasing DCP content to 1%, the recovery ratio reached 80%. Therefore, the driving force for the shape recovery at low temperature was related to the cross-linking structure.

To analyse the influences of DCP content on the shape memory performance, we further compared the "V" shape recovery process of the samples with different DCP contents (Fig. 8) at 45 °C by taking photos. With the content of DCP increasing, the recovery rate increased obviously. For example, the PLA/PPC blend without DCP had the lowest recovery degree at every moment compared with those samples with DCP. Therefore, the cross-link structure offered stronger recovery driving force and improved the recovery speed. For the samples with 1.5 wt% and 2 wt% of DCP, the difference of recovery rate was not obvious, which suggested that the excess cross-linking structure might limit the mobility of the chains and could not improve further the recovery performance.

Based on the above results, the relationship between the structure and the properties in PLA/PPC/DCP system can be illustrated by Scheme 2. In the system, DCP could initiate the cross-linking reaction between PLA and PPC chains and that among the two homopolymers themselves, as well as the degradation of PPC and PLA homopolymers. Therefore, there coexisted in PLA/PPC/DCP system cross-linked PLA and PPC, free PLA, free PPC and a small amount of cross-linked PLA or PPC homopolymer. However, among them, the cross-linked chains between PLA and PPC were dominant and supplied good interfacial adhesion and improved the mechanical properties of the PLA/PPC blends (Scheme 2a). In the shape memory process (Scheme 2b), both free PPC and PLA could recover at high temperature (above 55 °C). When the recovery temperature was below the T_g of PLA, for example at 45 °C, the recovery structure in PLA/PPC samples with DCP became very different from that without DCP. Without DCP, only PPC chains could recover at 45 °C and the *R*r was only 50%; however, with DCP, the recovery of PPC chains remained as it is, while the existence of chemical cross-linking structure between PLA and PPC chains could result in the recovery of PLA chains and the *R*r improved. Furthermore, the cross-linking structure with great elasticity enhanced the recovery driving force and increased the recovery rate. Therefore, the fully biodegradable shape memory polymers with recovery property at low temperature were obtained by *in situ* cross-linking reaction of PLA and PPC.

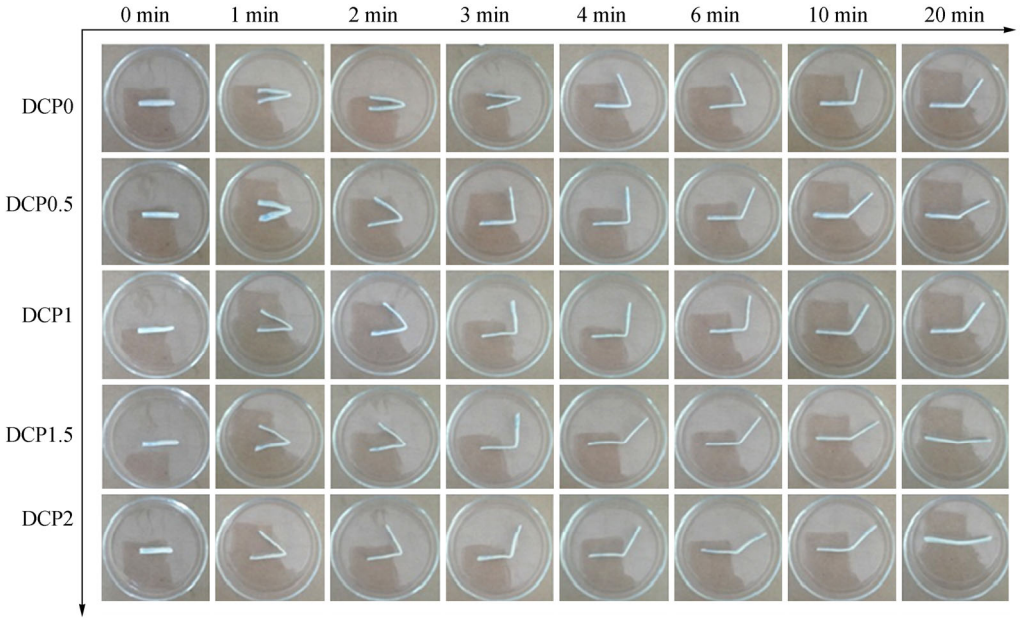

Fig. 8 "V" shape recovery process at 45 °C of the samples with different DCP contents recorded at different time

https://doi.org/10.1007/s10118-018-2065-3

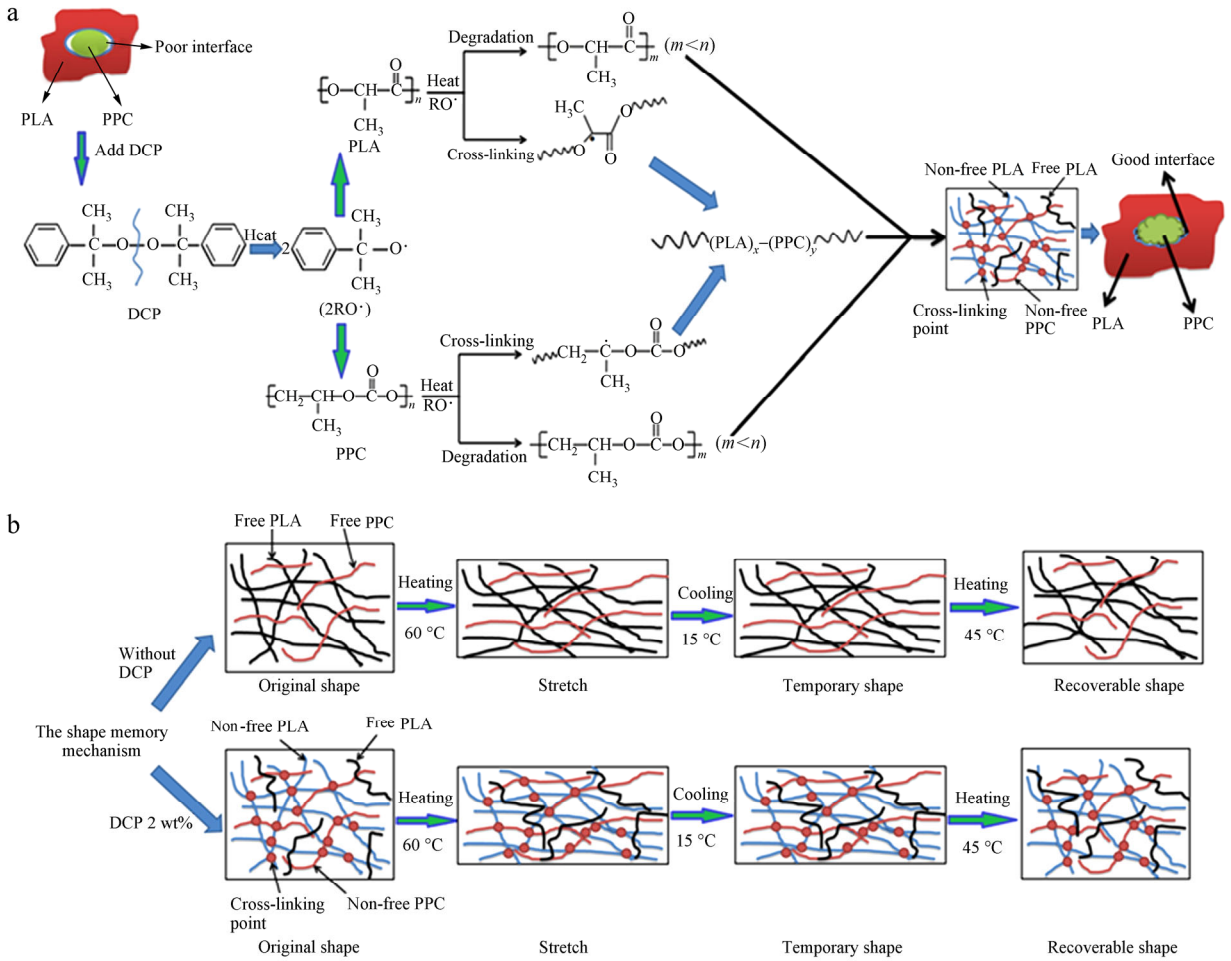

Scheme 2 Illustration of (a) the structure change of PLA/PPC blends caused by DCP and (b) their effects on the shape memory mechanism

CONCLUSIONS

Fully biodegradable PLA/PPC blends with good shape memory performance were prepared. Because of their similar chemical structures, cross-linking structure between PLA and PPC chains was obtained by *in situ* compatibilization by addition of DCP, which brought great change to the phase structure. When DCP content increased from 0 wt% to 2 wt%, the phase morphology changed from the "sea-island" structure to homogeneous phase structure. As a consequence, the elongation at break of PLA/PPC/DCP increased twice. Both the unchanged tensile strength and the peculiar change of T_g indicated the degradation of PPC and PLA homopolymers at the same time together with the cross-linking reaction. The investigation of shape memory performance demonstrated that the blends with DCP had good recovery performance at 45 °C and the recovery rate increased with the DCP content. Thus, the cross-linking structure between PLA and PPC decreased the shape recovery temperature to a lower value close to the body temperature. This study provides an effective method to obtain eco-friendly PLA/PPC blends with good mechanical performance and shape memory properties, which will promote the applications of biodegradable shape memory material in the medical fields.

ACKNOWLEDGMENTS

This work was financially supported by the National Natural Science Foundation of China (No. 51503117) and the Innovation Foundation for Graduate Students of Shandong University of Science and Technology, China (No. SDKDYC170334).

REFERENCES

1 Cha, K. J.; Lih, E.; Choi, J.; Joung, Y. K.; Ahn, D. J.; Han, D. K. Shape-memory effect by specific biodegradable polymer blending for biomedical applications. Macromol. Biosci. 2014, 14(5), 667–678.
2 Wong, Y. S.; Stachurski, Z. H.; Venkatraman, S. S. Modeling shape memory effect in uncrosslinked amorphous biodegradable polymer. Polymer 2011, 52(3), 874–880.
3 Kotharangannagari, V. K.; Krishnan, K. Biodegradable hybrid nanocomposites of starch/lysine and zno nanoparticles with shape memory properties. Mater. Design 2016, 109, 590–595.
4 Navarro-Baena, I.; Sessini, V.; Dominici, F.; Torre, L.; Kenny, J. M.; Peponi, L. Design of biodegradable blends based on PLA and PCL: from morphological, thermal and mechanical studies to shape memory behavior. Polym. Degrad. Stab. 2016, 132, 97–108.
5 Gu, S.; Gao, X.; Jin, S.; Liu, Y. Biodegradable shape memory polyurethanes with controllable trigger temperature. Chinese J. Polym. Sci. 2016, 34(6), 720–729.

6 Zini, E.; Scandola, M.; Dobrzynski, P.; Kasperczyk, J.; Bero, M. Shape memory behavior of novel (L-lactide-glycolide-trimethylene carbonate) terpolymers. Biomacromolecules 2009, 8(11), 3661–3667.
7 Xing, Q.; Li, R.; Dong, X.; Zhang, X.; Zhang, L.; Wang, D. Phase morphology, crystallization behavior and mechanical properties of poly(L-lactide) toughened with biodegradable polyurethane: effect of composition and hard segment ratio. Chinese J. Polym. Sci. 2015, 33(9), 1294–1304.
8 Talbamrung, T.; Kasemsook, C.; Sangtean, W.; Wachirahuttapong, S.; Thongpin, C. Effect of peroxide and organoclay on thermal and mechanical properties of PLA in PLA/NBR melted blend. Energy. Proced. 2016, 89, 274–281.
9 Jing, X.; Mi, H.; Peng, X.; Turng, L. The morphology, properties, and shape memory behavior of polylactic acid/thermoplastic polyurethane blends. Polym. Eng. Sci. 2015, 55(1), 70–80.
10 Wei, Z.; Long, C.; Yu, Z. Surprising shape-memory effect of polylactide resulted from toughening by polyamide elastomer. Polymer 2009, 50(5), 1311–1315.
11 Yuan, D.; Chen, Z.; Xu, C.; Chen, K.; Chen, Y. Fully biobased shape memory material based on novel cocontinuous structure in poly(lactic acid)/natural rubber TVPs fabricated *via* peroxide-induced dynamic vulcanization and *in situ* interfacial compatibilization. ACS Sustain. Chem. Eng. 2015, 3(11), 2856–2865.
12 Barreto, C.; Altskär, A.; Fredriksen, S.; Hansen, E.; Rychwalski, R. W. Multiwall carbon nanotube/ppc composites: preparation, structural analysis and thermal stability. Eur. Polym. J. 2013, 49(8), 2149–2161.
13 Wang, X. Y.; Weng, Y. X.; Wang, W.; Huang, Z. G.; Wang, Y. Z. Modification of poly(propylene carbonate) with chain extender ADR-4368 to improve its thermal, barrier, and mechanical properties. Polym. Test 2016, 54, 301–307.
14 Xing, C.; Wang, H.; Hu, Q.; Xu, F.; Cao, X.; You, J. Mechanical and thermal properties of eco-friendly poly(propylene carbonate)/cellulose acetate butyrate blends. Carbohyd. Polym. 2013, 92(2), 1921–1927.
15 Hu, X.; Xu, C.; Gao, J.; Yang, G.; Geng, C.; Chen, F. Toward environment-friendly composites of poly(propylene carbonate) reinforced with cellulose nanocrystals. Compos. Sci. Technol. 2013, 78(2), 63–68.
16 Cui, S.; Li, L.; Wang, Q. Enhancing glass transition temperature and mechanical properties of poly(propylene carbonate) by intermacromolecular complexation with poly(vinyl alcohol). Compos. Sci. Technol. 2016, 127, 177–184.
17 Seo, J.; Jeon, G.; Jang, E. S.; Khan, S. B.; Han, H. Preparation and properties of poly(propylene carbonate) and nanosized zno composite films for packaging applications. J. Appl. Polym. Sci. 2011, 122(2), 1101–1108.
18 Song, P.; Xiao M.; Du, F.; Wang, S.; Gan, L.; Liu, G. Synthesis and properties of aliphatic polycarbonates derived from carbon dioxide, propylene oxide and maleic anhydride. J. Appl. Polym. Sci. 2008, 109(6), 4121–4129.
19 Wang, S., Du, L., Zhao, X., Meng, Y., Tjong, S. Synthesis and characterization of alternating copolymer from carbon dioxide and propylene oxide. J. Appl. Polym. Sci. 2010, 85(11), 2327–2334.
20 Li, Z.; Li, W.; Zhang, H.; Dong, L. Thermal, rheological and mechanical properties of poly(propylene carbonate)/methyl methacrylate-butadiene-styrene blends. Iran. Polym. J. 2015, 24(10), 861–870.
21 Zhou, L.; Zhao, G.; Jiang, W. Effects of catalytic transesterification and composition on the toughness of poly(lactic acid)/poly(propylene carbonate) blends. Ind. Eng. Chem. Res. 2016, 55(19), 5565–5573.
22 Chen, Y.; Peng, Y.; Liu, W.; Zeng, G.; Li, X.; Yan, X. Study on the mechenical properties of PPC/PLA blends modified by poss. Adv. Mater. Res. 2013, 741, 28–32.
23 Gao, J.; Fu, Q.; Bai, H.; Zhang, Q. Effect of homopolymer poly(vinyl acetate) on compatibility and mechanical properties of poly(propylene carbonate)/poly(lactic acid) blends. Express Polym. Lett. 2012, 6(11), 860–870.
24 Yao, M.; Deng, H.; Mai, F.; Wang, K. Modification of poly(lactic acid)/poly(propylene carbonate) blends through melt compounding with maleic anhydride. Express Polym. Lett. 2011, 5(11), 937–949.
25 Hwang, S. W.; Park, D. H.; Kang, D. H.; Lee, S. B.; Shim, J. K. Reactive compatibilization of poly(L-lactic acid)/poly(propylene carbonate) blends: thermal, thermomechanical, and morphological properties. J. Appl. Polym. Sci. 2016, 133(18), DOI: 10.1002/APP.43388
26 Yuan, D.; Xu, C.; Chen, Z.; Chen, Y. Crosslinked bicontinuous biobased polylactide/natural rubber materials: super toughness, “net-like”-structure of NR phase and excellent interfacial adhesion. Polym. Test 2014, 38, 73–80.
27 Xu, P.; Ma, P.; Cai, X.; Song, S.; Zhang, Y.; Dong, W. Selectively cross-linked poly (lactide)/ethylene-glycidyl methacrylate-vinyl acetate thermoplastic elastomers with partial dual-continuous network-like structures and shape memory performances. Eur. Polym. J. 2016, 84, 1–12.
28 Raidt, T.; Hoeher, R.; Katzenberg, F.; Tiller, J. C. Chemical cross-linking of polypropylenes towards new shape memory polymers. Macromol. Rapid Commun. 2015, 36(8), 744–749.
29 Wang, Y.; Zhu, G.; Tang, Y.; Xie, J.; Liu, T.; Liu, Z. Mechanical and shape memory behavior of chemically cross-linked SBS/LDPE blends. J. Polym. Res. 2014, 21(4), 1–10.
30 Ma, P.; Cai, X.; Zhang, Y.; Wang, S.; Dong, W.; Chen, M.; Lemstra, P. J. *In situ* compatibilization of poly(lactic acid) and poly(butylene adipate-*co*-terephthalate) blends by using dicumyl peroxide as a free-radical initiator. Polym. Degrad. Stab. 2014, 102(2), 145–151.
31 Akos, N. I.; Wahit, M. U.; Mohamed, R.; Yussuf, A. A. Preparation, characterization, and mechanical properties of poly(*ε*-caprolactone)/polylactic acid blend composites. Polym. Compos. 2013, 34(5), 763–768.
32 Rytlewski, P.; Żenkiewicz, M.; Malinowski, R. Influence of dicumyl peroxide content on thermal and mechanical properties of polylactide. Int. Polym. Proc. 2013, 26(5), 580–586.
33 Lim, S. W.; Choi, M. C.; Jeong, J. H.; Park, E. Y.; Ha, C. S. Toughening poly(lactic acid) (PLA) through reactive blending with liquid polybutadiene rubber (LPB). Compos. Interface. 2016, 23(8), 807–818.
34 Agarwal, M.; Koelling, K. W.; Chalmers, J. J. Characterization of the degradation of polylactic acid polymer in a solid substrate environment. Biotechnol. Prog. 1998,14(3), 517–526.
35 Fei, B.; Chen, C.; Peng, S.; Zhao, X.; Wang, X.; Dong, L. FTIR study of poly(propylene carbonate)/bisphenol A blends. Polym. Int. 2010, 53(12), 2092–2098.

https://doi.org/10.1007/s10118-018-2065-3